https://ieeexplore.ieee.org/abstract/document/7799311

DOI: 10.1109/CDC.2016.7799311

Model predictive control of large-scale urban networks via perimeter control and route guidance actuation

Isik Ilber Sirmatel and Nikolas Geroliminis

***Abstract*— We design model predictive control (MPC) schemes to improve urban mobility in heterogeneously congested large-scale traffic networks, the modeling and control of which remains a challenge. The multi-region urban network is modeled using the macroscopic fundamental diagram (MFD) of urban traffic, with each region having a well-defined MFD. For more realistic simulations of urban networks with route guidance actuation based control, we propose a new model with cyclic behavior prohibition. Furthermore, we extend upon earlier work on perimeter control based MPC schemes with MFD modeling by integrating route guidance type actuation, which distributes flows exiting a region over its neighboring regions. Performance of the proposed schemes are evaluated via simulations of a congested scenario with noise in demand estimation and measurement errors. Results show the possibility of substantial improvements in urban network performance.**

I. INTRODUCTION

Modeling and control of large-scale urban traffic networks present considerable challenges. Inadequate infrastructure and coordination, spatiotemporal propagation of congestion, and the uncertainty in traveler choices contribute to the difficulties faced when creating realistic models and designing effective traffic control schemes for urban networks. Although considerable research has been directed towards designing efficient real-time traffic control schemes in the last decades (see [1] for a review), control design for heterogeneously congested large-scale urban networks remains a challenging problem.

Traffic modeling and control studies for urban networks usually focus on microscopic models keeping track of link-level traffic dynamics with control strategies using local information. Based on the linear-quadratic regulator (LQR) problem, traffic-responsive urban control (TUC) [2] and its extensions [3], [4] represent a multivariable feedback regulator approach for network-wide urban traffic control. Although TUC can deal with oversaturated conditions via minimizing and balancing the relative occupancies of network links, it may not be optimal for heterogeneous networks with multiple pockets of congestion. Inspired by the max pressure routing scheme for wireless networks [5], many local traffic control schemes have been proposed for networks of signalized intersections (see [6]–[9]), which involve evaluations at each intersection requiring information exclusively from adjacent links. Although the high accuracy of microscopic traffic models is desirable for simulation purposes, the increased model complexity results in complications for control, whereas local control strategies might not be able to operate properly under heavily congested conditions, as they do not protect the congested regions upstream. Another disadvantage of sophisticated local controllers is that they might require detailed information on traffic states, which are difficult to estimate or measure.

An alternative to local real-time traffic signal control methods is the two layer hierarchical control approach. At the upper layer, the network-level controller optimizes network performance via regulating macroscopic traffic flows through interregional actuation systems (e.g., perimeter control), whereas at the lower layer the local controllers regulate microscopic traffic movements through intraregional actuation systems (e.g., signalized intersections). The macroscopic fundamental diagram (MFD) of urban traffic is a modeling tool for developing low complexity aggregated dynamic models of urban networks, which are required for the design of efficient network-level control schemes for the upper layer. It is possible to model an urban region with roughly homogeneous accumulation (i.e., small spatial link density heterogeneity) with an MFD, which provides a unimodal, low-scatter, and demand-insensitive relationship between accumulation and trip completion flow [10].

The concept of MFD with an optimum accumulation was first proposed by Godfrey [11], and its existence was recently verified with dynamic features and real data in [10]. Control strategies based on MFD modeling and using perimeter control type actuation have been proposed by many researchers for single-region (see [12]–[15]) and multi-region (see [16], [17]) urban areas. Application of the MPC technique to the control of urban networks with MFD modeling also attracted recent interest. In [18], the authors design a nonlinear MPC for a simple two-region urban network equipped with a perimeter control system. The work in [19] generalizes the two-region MFD network model of [18] to that of an R-region network, and proposes hybrid MPC schemes for an urban network equipped with both perimeter control systems and switching signal timing plans. For the cooperative control of a mixed transportation network consisting of a freeway and two urban regions, an MPC scheme is proposed in [20]. A model capturing the dynamics of heterogeneity is developed in [21], alongside a hierarchical control system with MPC on the upper level. More detailed literature reviews in local traffic control, MFD modeling, and MFD based control can be found in [3], [7], and [21]. These recent studies on perimeter control based MPC schemes for urban networks do not explore any opportunity for manipulating the routes of the drivers through

Isik Ilber Sirmatel and Nikolas Geroliminis are with the School of Architecture, Civil and Environmental Engineering, École Polytechnique Fédérale de Lausanne (EPFL), 1015 Lausanne, Switzerland. {isik.sirmatel,nikolas.geroliminis}@epfl.ch

feedback control via actuation with route guidance systems. Although there are also some recent attempts at developing traffic control schemes with route guidance capability (see [22], [23],) the integration of perimeter control and route guidance type actuation still remains unexplored.

In this work we first introduce a new urban network model capable of expressing aggregated traffic dynamics via MFDs, while at the same time avoiding cyclic behavior (i.e., prohibiting vehicles from flowing back and forth between neighboring regions), which is where it differs from similar MFD-based urban network models. Furthermore, we design network-level nonlinear MPC schemes for a heterogeneous urban traffic network with a given partition into homogeneous regions (see fig. 1), each with a well-defined MFD. We extend upon earlier works that propose perimeter control actuation based MPC schemes for urban networks by integrating the route guidance type actuation in the MPC formulation. In congested conditions drivers tend to take longer routes, leading to increased traveled distances and thus also higher emissions. Results show that the MPC schemes are capable of decreasing both the delays (time spent in traffic) and traveled distance at the same time, suggesting substantial potential in improving urban mobility.

II. MFD-BASED MODELING OF URBAN NETWORKS

We consider an urban network $\mathcal{R}$ with heterogeneous distribution of accumulation, consisting of R homogeneous regions, i.e., $\mathcal{R} = \{1, 2, \dots, R\}$, each with a well-defined MFD. A network consisting of 7 regions is schematically shown in fig. 1. The exogenous traffic flow demand generated in region i with destination region j is denoted by $q_{ij}(t)$ (veh/s), whereas $n_{ij}(t)$ (veh) denotes the vehicle accumulation in region i with destination region j, and $n_i(t)$ (veh) the total accumulation in region i, at time t; $i, j \in \mathcal{R}$; $n_i(t) = \sum_{j\in\mathcal{R}} n_{ij}(t)$. Between each pair of neighboring regions i and h ($i \in \mathcal{R}$, $h \in \mathcal{N}_i$, where $\mathcal{N}_i$ is the set of regions neighboring region i) there exists perimeter control type actuators $u_{ih}(t)$ and $u_{hi}(t)$ (–), $u_{ih}(t), u_{hi}(t) \in [0, 1]$, that can manipulate the transfer flows between regions i and h. Furthermore, each region i is assumed to be equipped with route guidance type actuators $\theta_{ihj}(t)$ ($i \in \mathcal{R}$, $h \in \mathcal{N}_i$, $j \in \mathcal{R} \setminus \{i\}$), that can distribute the transfer flows with destination region j exiting region i over its neighboring regions h, with $\sum_{h\in\mathcal{N}_i} \theta_{ihj}(t) = 1$.

Dynamics of an R-region MFDs network can be written as (based on the work in [21] and [22])

$$\dot{n}_{ii}(t) = q_{ii}(t) - M_{ii}(t) + \sum_{h\in\mathcal{N}_i} u_{hi}(t)\hat{M}_{hii}(t), \quad (1a)$$

$$\dot{n}_{ij}(t) = q_{ij}(t) - \sum_{h\in\mathcal{N}_i} u_{ih}(t)\hat{M}_{ihj}(t) + \sum_{h\in\mathcal{N}_i; h\neq j} u_{hi}(t)\hat{M}_{hij}(t), \quad (1b)$$

for $i, j \in \mathcal{R}$, $i \neq j$, where $\hat{M}_{ihj}(t)$ (veh/s) is the effective transfer flow from region i with destination j through the next immediate region h, which is calculated as [22]

$$\hat{M}_{ihj}(t) = \min\left(M_{ihj}(t), c_{ih}(n_h(t))\frac{n_{ij}(t)\theta_{ihj}(t)}{\sum_{k\in\mathcal{R}} n_{ik}(t)\theta_{ihk}(t)}\right), \quad (2)$$

where $M_{ihj}(t)$ and $\theta_{ihj}(t)$ denote the transfer flow and the percentage of outflow, respectively, from region i to destination region j through the next immediate region h, and $c_{ih}(n_h(t))$ is the boundary capacity between regions i and h that depends on the accumulation in region h. The boundary capacity constraint can be omitted in the prediction model inside MPC for computational advantage. The physical reasoning of this omission is that (i) the boundary capacity decreases for accumulations much larger than the critical accumulation, and (ii) the controller will not allow the regions to have accumulations close to gridlock [20]. With this omission, the transfer flow $M_{ihj}(t)$ is used in the prediction model given in (1) instead of the effective transfer flow $\hat{M}_{ihj}(t)$, and is calculated corresponding to the ratio between accumulations as

$$M_{ihj}(t) = \theta_{ihj}(t)\frac{n_{ij}(t)}{n_i(t)}G_i(n_i(t)), \quad (3)$$

where $G_i(n_i(t))$ (veh/s) is the trip completion flow (i.e., outflow) of region i at accumulation $n_i(t)$, defining the MFD of region i. It is assumed that all trips inside a region have similar lengths (i.e., the distance traveled per vehicle inside a region does not depend on the origin and destination of the trip). Simulation and empirical results [10] suggest that the MFD can be approximated by an asymmetric unimodal curve skewed to the right (i.e., the critical accumulation, which maximizes $G_i(n_i(t))$, is smaller than half of the jam accumulation $n_{i,\text{jam}}$, which puts the region in gridlock). Thus, $G_i(n_i(t))$ can be expressed with a third-order polynomial in the variable $n_i(t)$, e.g. $G_i(n_i(t)) = a_i n_i^3(t) + b_i n_i^2(t) + c_i n_i(t)$, where a_i, b_i, and c_i are estimated parameters.

The urban network model (1) has no memory of where the vehicles were previously, thus does not prohibit vehicles from flowing back and forth between neighboring regions (i.e., it permits cyclic behavior), leading to unrealistic

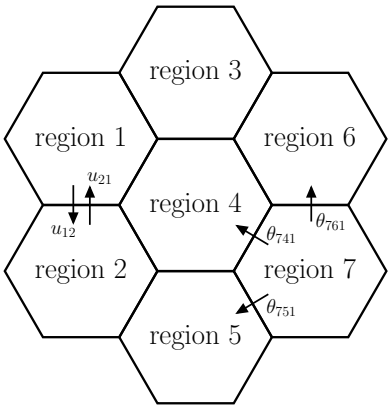

Fig. 1. Schematic of an urban network with 7 regions.

simulations. While this memoryless choice of routes (i.e., sequence of regions) is not crucial when only perimeter control actuation is applied, it is important for route guidance based schemes, where the controller tries to emulate perimeter control actuation via cyclic routes. For avoiding cyclic behavior, we propose the following urban network model:

$$\dot{n}_{iiii}(t) = q_{ii}(t) - M_{iiii}(t),\ \forall i \in \mathcal{R}, \tag{4a}$$

$$\dot{n}_{iiij}(t) = q_{ij}(t) - \sum_{h \in \mathcal{N}_i} u_{ih}(t)\tilde{M}_{ofgij}(t), \quad \forall i,j \in \mathcal{R},\ j \neq i, \tag{4b}$$

$$\dot{n}_{ogii}(t) = \sum_{f \in \mathcal{N}_g^* \setminus \{i\}} u_{gi}(t)\tilde{M}_{ofgii}(t) - M_{ogii}(t), \quad \forall o,g,i \in \mathcal{R},\ g \in \mathcal{N}_i,\ o \neq i, \tag{4c}$$

$$\dot{n}_{ogij}(t) = \sum_{f \in \mathcal{N}_g^* \setminus \{i,j\}} u_{gi}(t)\tilde{M}_{ofgij}(t) - \sum_{h \in \mathcal{N}_i \setminus \{o,g\}} u_{ih}(t)\tilde{M}_{ogihj}(t), \quad \forall o,g,i,j \in \mathcal{R},\ g \in \mathcal{N}_i,\ o \neq i,\ o \neq j,\ g \neq j,\ j \neq i, \tag{4d}$$

where $n_{ogij}(t)$, $M_{ogij}(t)$, and $\theta_{ogihj}(t)$ denote the accumulation in region i, transfer flow from region i, and the percentage of outflow from region i, respectively, with origin region o, immediately preceding region g, destination region j, and, for $\theta_{ogihj}(t)$, through the next immediate region h, $\mathcal{N}_g^*$ is the set containing regions neighboring region g and region g itself, and the distributed transfer flow $\tilde{M}_{ogihj}(t)$ is defined as

$$\tilde{M}_{ogihj}(t) = \theta_{ogihj}(t)M_{ogij}(t), \tag{5}$$

with $M_{ogij}(t)$ defined as

$$M_{ogij}(t) = \frac{n_{ogij}(t)}{n_i(t)}G_i(n_i(t)). \tag{6}$$

Using the model (4) for simulations with MPC controllers having (1) as the prediction model requires the transfer of variables between the two models as follows:

$$n_{ij}(t) = \sum_{o \in \mathcal{R}\setminus\{j\}} \sum_{g \in \mathcal{R}\setminus\{j\}} n_{ogij}(t),\ \forall i,j \in \mathcal{R},$$

$$\theta_{ihj}(t) = \theta_{ogihj}(t),\ \forall o,g,i,j \in \mathcal{R},\ g \in \mathcal{N}_i,\ h \in \mathcal{N}_i \setminus \{o,g\}\ o \neq i,\ o \neq j,\ g \neq j,\ j \neq i.$$

The model (4) prohibits cyclic behavior of length two (e.g., for fig. 1, a route of $1-2-1$ is prohibited, whereas a route of $1-2-4-1$ is allowed), thus it is a more realistic representation of urban network dynamics. For prohibiting longer cycles, (4) should be extended with longer route memory, but this is not considered in this work since cycles longer than two are assumed to be negligible. The model (4) is used as the simulation model (i.e., the *plant*) in the case studies, whereas (1) is used as the prediction model for computational advantage.

III. MPC SCHEMES WITH PERIMETER CONTROL AND ROUTE GUIDANCE ACTUATION

We formulate the problem of finding the u_{ih} and θ_{ihj} values that minimize the total network delay (i.e., total time spent in the network) as the following finite horizon constrained optimal control problem:

$$\begin{aligned}
&\text{minimize} \quad \sum_{i=1}^{R}\sum_{j=1}^{R}\int_{t_c}^{t_c+T} n_{ij}(t)dt \qquad (8)\\
&\text{subject to}\\
&n_{ij}(t_c) = \hat{n}_{ij}(t_c),\ \forall i,j \in \mathcal{R}\\
&\forall t \in [t_c, t_c+T]:\\
&\quad \text{Model equations (1) and (3)},\ \forall i,j \in \mathcal{R}\\
&\quad 0 \leq \sum_{j \in \mathcal{R}} n_{ij}(t) \leq n_{i,\text{jam}},\ \forall i \in \mathcal{R}\\
&\quad u_{\min} \leq u_{ih}(t) \leq u_{\max},\ \forall i \in \mathcal{R}, h \in \mathcal{N}_i\\
&\quad 0 \leq \theta_{ihj}(t) \leq 1,\ \forall i,j \in \mathcal{R}, i \neq j, h \in \mathcal{N}_i\\
&\quad \sum_{h \in \mathcal{N}_i} \theta_{ihj}(t) = 1,\ \forall i,j \in \mathcal{R}, i \neq j,
\end{aligned}$$

where t_c is the current control sampling instant in time and $\hat{n}_{ij}(t_c)$ is the measurement taken at that instant, T is the prediction horizon, $n_{i,\text{jam}}$ is the jam accumulation for region i, whereas $u_{\min}$ and $u_{\max}$ are the lower and upper bounds of the perimeter control input u_{ih}.

To be able to solve (8) numerically, we resort to approximating it as a finite dimensional nonlinear program (NLP) via direct methods. The resulting NLP is nonconvex due to the nonlinear prediction model, and as such can be solved via NLP solvers that are able to treat nonconvex problems.

We propose three MPC schemes: (i) perimeter control MPC (MPC_{PC}), (ii) route guidance MPC (MPC_{RG}), (iii) perimeter control and route guidance MPC (MPC_{PCRG}), each with a different set of available actuator types. MPC_{PC} and MPC_{RG} schemes solve variants of the optimization problem given in (8) in receding horizon, each with different conditions on $u_{ih}(t_c)$ and $\theta_{ihj}(t_c)$, whereas MPC_{PCRG} solves exactly the MPC problem as given in (8). The MPC_{PC} scheme has access to the perimeter control type actuation only, while drivers are left free to choose their own routes. Thus, for this scheme, only the perimeter control commands $u_{ih}(t_c)$ are the control inputs, whereas route guidance commands $\theta_{ihj}(t_c)$ are assumed to be known (this assumption will be relaxed and further investigated in an extended version of this work). In contrast to the MPC_{PC} scheme, MPC_{RG} has access to the route guidance type actuation only, while perimeter control commands are fixed to $u_{\max}$. Thus, for the MPC_{RG} scheme, the route guidance commands $\theta_{ihj}(t_c)$ are the only control inputs. Finally, the MPC_{PCRG} scheme has access to both the perimeter control and route guidance type actuators, thus both types of commands are the control inputs.

IV. CASE STUDIES

A. Network Description and Simulation Setup

All simulations are conducted on a 7 region urban network having the structure given in fig. 1, with the simulation

model given in (4) for representing the reality. Each region is assumed to have the same MFD, with the MFD parameters $a_i = 1.4877 \cdot 10^{-7}/3600$, $b_i = -2.9815 \cdot 10^{-3}/3600$, $c_i = 15.0912/3600$, jam accumulation $n_{i,\text{jam}} = 10^4$ (veh), critical accumulation $n_{i,\text{cr}} = 3.4 \cdot 10^3$ (veh), and maximum outflow $G_i(n_{i,\text{cr}}) = 6.3$ (veh/s), which are consistent with the MFD observed in a part of downtown Yokohama (see [10]), which has an area of approximately 10 km^2.

Simulation-based studies, with the MPC schemes implemented via the CasADi toolbox [24] in MATLAB, calling the solver IPOPT [25], revealed that direct single shooting for the MPC$_{\text{PC}}$, and direct collocation for the MPC$_{\text{RG}}$ and MPC$_{\text{PCRG}}$ schemes, give the best results in terms of computational efficiency, thus these methods are chosen for the case studies. A numerical integrator based on the RK4 method is used in single shooting, whereas a Legendre polynomial of degree 3 is used for polynomial interpolation in collocation. Furthermore, prediction horizon is chosen as $T = 20$ minutes, whereas the horizon is split into $N = 5$ control intervals. Simulation and control sampling times are 30 s and 240 s, while the length of the simulation experiment is $T_exp = 240$ (in number of simulation steps), giving an effective length of 120 minutes. Bounds of the perimeter control commands are $u_{\min} = 0.1$ and $u_{\max} = 0.9$. Move blocking is employed in the formulations to reduce computational effort, with the moves after the first one blocked. To avoid abrupt changes in control inputs, rate limiting is employed with the rate limit chosen as 0.2 between two consecutive control steps, for both control inputs. Studies into how the control configuration influences performance and computational effort will be included in an extended version of this work.

For capturing the effect of measurement noise in accumulation states, we add random noise terms with normal distribution to the measured states:

$$\tilde{n}_{ij}(t) = n_{ij}(t) + n_{ij}(t) \cdot \mathcal{N}(0, \sigma^2_{n_{ij}}), \ \forall i, j \in \mathcal{R}, \quad (9)$$

where the noise has zero mean and its variance is chosen as $\sigma^2_{n_{ij}} = 0.25$ in the simulations. Furthermore, the uncertainty in demands is also considered, with the MPC schemes having access to average demand profiles whereas the actual flow demands driving the simulation model are assumed to have zero mean random noise terms:

$$\tilde{q}_{ij}(t) = q_{ij}(t) + q_{ij}(t) \cdot \mathcal{N}(0, \sigma^2_{q_{ij}}), \ \forall i, j \in \mathcal{R}, \quad (10)$$

with the variance chosen as $\sigma^2_{q_{ij}} = 0.25$ in the simulations, representing presence of large noise.

Performance metrics are *sum of total time spent* (STTS, veh·s) and *sum of total traveled distance* (STTD, veh·m), which are defined for a single simulation experiment as follows:

$$\text{STTS} = T_s \cdot \sum_{t=1}^{T_{\text{exp}}} \sum_{i \in \mathcal{R}} n_i(t), \quad (11)$$

$$\text{STTD} = T_s \cdot \sum_{t=1}^{T_{\text{exp}}} \sum_{i \in \mathcal{R}} l_i \cdot \left(M_{ii}(t) + \sum_{h \in \mathcal{N}_i} \sum_{j \in \mathcal{R} \setminus i} Q_{ihj}(t) \right), \quad (12)$$

where l_i is the average trip length of trips inside region i, assumed constant and chosen as 3600 m for all regions, whereas $Q_{ihj}(t)$ is defined as $Q_{ihj}(t) = u_{ih}(t)\theta_{ihj}(t)M_{ij}(t)$.

The MPC controllers are compared with a *no control* (NC) case, in which the perimeter control commands $u_{ih}(t_c)$ are fixed to $u_{\max}$, while drivers are left free to choose their routes. In simulations this is captured by calculating the $\theta_{ihj}(t_c)$ values by a logit model (see [26]) using the current travel times from region i to destination region j through the K_{SP} shortest sequences of regions connecting the two, calculated with Dijkstra's algorithm. As drivers adapt to traffic conditions in real time, the $\theta_{ihj}(t_c)$ values are updated at each control step. The logit model relaxes the assumption that drivers always choose the physical shortest path. Simulations with route choices calculated via logit model thus tend to be more realistic because drivers rarely have perfect information and do not always behave as rational actors. The parameters of the logit model can be adjusted to reflect the amount of information available to drivers (or sensitivity of drivers to differences in travel time between routes).

B. Congested Scenario

In this case study the network is uncongested at the beginning but faces increased flow demands as time progresses. The results are given in fig. 2, where the evolution of regional accumulations are shown alongside graphs of total time spent, cumulative traveled distance, outflow of city center (i.e., region 4), and the noisy flow demands $\tilde{q}_{ij}(t)$, all as a function of simulation time, for the no control (NC) case and the three MPC schemes. A summary of the results is given in table I, which shows that all MPC schemes are capable of improving mobility of the urban network, as they have decreased values of both the STTS and STTD metrics, in comparison to the NC case.

Compared to the other two MPC schemes, MPC$_{\text{PCRG}}$ is superior in distributing the vehicle flows efficiently over the whole network, which translates to efficient usage of the network capacity, leading to less congestion and also decreased values of STTS. This is clearly seen in the regional accumulation plots (b)–(d) in fig. 2, where MPC$_{\text{PCRG}}$ can suppress congestion evenly in all regions, whereas MPC$_{\text{RG}}$ cannot avoid congestion in region 2 due to lack of perimeter control authority, although it is successful in managing the rest of the network. MPC$_{\text{PC}}$, on the other hand, can use its

TABLE I
PERFORMANCE EVALUATION FOR CONGESTED SCENARIO

Control scheme	STTS ($\times 10^7$ veh·s)	STTS imprv. over NC (%)	STTD ($\times 10^8$ veh·m)	STTD imprv. over NC (%)	Avg. CPU time (s)	Max. CPU time (s)
NC	9.53	–	4.97	–	–	–
MPC$_{\text{PC}}$	8.19	14	4.88	2	1.27	1.59
MPC$_{\text{RG}}$	7.00	27	4.61	7	5.65	6.11
MPC$_{\text{PCRG}}$	6.54	31	4.41	11	6.51	7.21

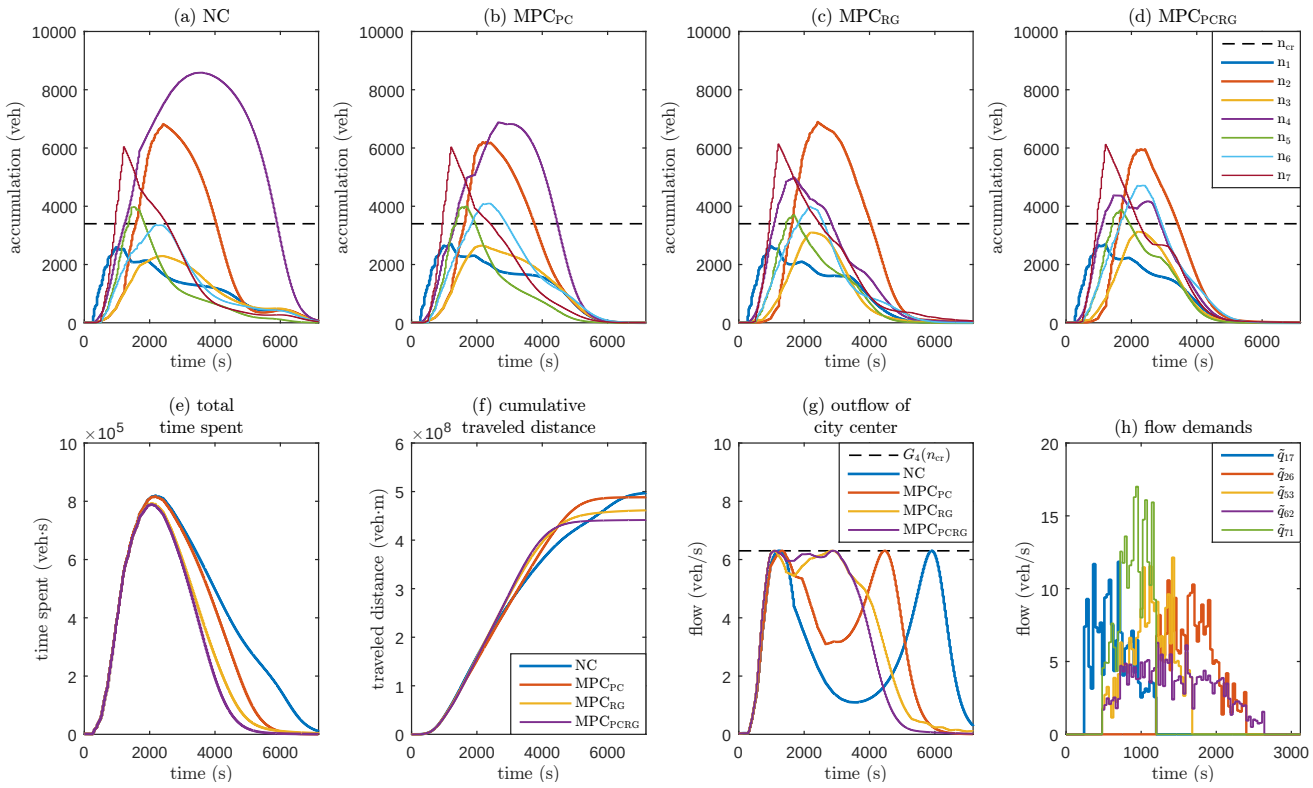

Fig. 2. Results of the congested scenario for the no control (NC) case and the three MPC schemes. Regional accumulations for (a) NC, (b) MPC$_{PC}$, (c) MPC$_{RG}$, (d) MPC$_{PCRG}$. Comparison of the four cases for (e) total time spent, (f) cumulative traveled distance, (g) outflow of city center. (h) Noisy flow demand profiles, expressing demands for trips between 5 origin-destination region pairs.

perimeter control authority efficiently to avoid congestion in all regions, but lacking the authority to manage routes, it cannot distribute traffic as efficiently as MPC$_{PCRG}$. Noting that control sampling time is chosen as 240 s, the computation time results[1] given in table I suggest that these schemes are computationally tractable, since their CPU times are negligible in comparison to the control sampling time.

The no control case cannot avoid heavy congestion close to gridlock in the city center, as seen in fig. 2 (a), leading to drastic decrease in outflow for the city center and thus inefficient use of the city center capacity for transferring flows from periphery to periphery. This is crucial for both STTS and STTD metrics, since routes through the city center are generally the physical shortest paths connecting two opposing peripheral regions. The MPC schemes, on the other hand, make efficient use of the city center, as seen in the city center outflow (i.e., $G_4(n_4(t))$) plot (g) in fig. 2, which shows that they succeed in keeping the city center close to critical accumulation n_{cr} (thus, operating close to maximum outflow $G_4(n_{cr})$) until network starts to unload.

The fact that route guidance based schemes can improve both STTS and STTD metrics, compared to the MPC$_{PC}$ scheme, stems from their authority over choosing routes for the vehicles, resulting in an increase in the percentage of drivers using the physical shortest path, as this would mean they spend less time (thus, lower STTS) and travel for shorter distances (thus, lower STTD) before reaching their destination and leaving the network. The percentage of drivers that are momentarily using the physical shortest path to their destinations is given in fig. 3 for the different schemes, which shows that route guidance based schemes succeed in making more drivers use the shortest path for their trips, explaining the improvement in STTD.

C. Effect of Driver Compliance

In an ideal case with route guidance, all drivers would follow the commands $\theta_{ihj}(t_c)$ exactly, but this may not be the case in reality as some drivers might prefer choosing their own routes instead of complying. To analyze how this

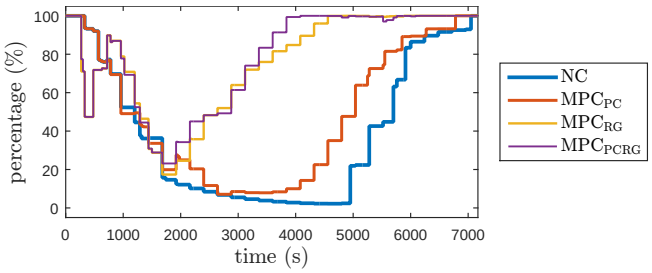

Fig. 3. Usage of physical shortest path for the congested scenario.

[1]These CPU times were obtained by calling IPOPT [25] from the CasADi toolbox [24] in MATLAB 8.5.0 (R2015a), on a 64-bit Windows PC with 3.6-GHz Intel Core i7 processor and 16-GB RAM.

TABLE II

STTS ($\times 10^7$ VEH·S) AND STTD ($\times 10^8$ VEH·M) VALUES FOR VARYING DRIVER COMPLIANCE LEVEL

Control scheme	Driver compliance level				
	10%	30%	50%	70%	90%
MPC_{RG} (STTS)	8.96	7.88	7.20	6.69	6.49
MPC_{PCRG} (STTS)	8.31	7.65	7.07	6.64	6.41
MPC_{RG} (STTD)	4.96	4.83	4.66	4.51	4.44
MPC_{PCRG} (STTD)	4.91	4.79	4.63	4.49	4.40

affects performance of the route guidance based schemes, a series of simulations, based on the congested scenario, are conducted by varying compliance from 10% to 90%. The results, given in table II, show that for levels beyond 50%, performance of the route guidance based MPC schemes are fairly insensitive to changes in driver compliance.

V. CONCLUSION

In this paper we proposed (a) a new urban network model with prohibition of cyclic behavior for more realistic MFD-based simulations of route guidance based schemes, (b) network-level perimeter control and route guidance based nonlinear MPC schemes via MFD modeling of heterogeneous urban networks, and demonstrated the possibility of substantial improvements in urban mobility through their use.

Future work will include (a) detailed studies into how the control configuration influences performance and computational effort, (b) development of hybrid MPC formulations of the proposed schemes for computational advantage, (c) comparison of the proposed schemes with other approaches (e.g., perimeter control based feedback control [17]), (d) more realistic simulation experiments with micro- or mesoscopic methods. Another interesting direction could be to explore methods for designing local traffic management schemes for enabling the implementation of the route guidance commands $\theta_{ihj}(t_c)$ in a real setting.

REFERENCES

[1] M. Papageorgiou, C. Diakaki, V. Dinopoulou, A. Kotsialos, and Y. Wang, "Review of road traffic control strategies," *Proceedings of the IEEE*, vol. 91, no. 12, pp. 2043–2067, 2003.

[2] C. Diakaki, M. Papageorgiou, and K. Aboudolas, "A multivariable regulator approach to traffic-responsive network-wide signal control," *Control Engineering Practice*, vol. 10, no. 2, pp. 183–195, 2002.

[3] K. Aboudolas, M. Papageorgiou, A. Kouvelas, and E. Kosmatopoulos, "A rolling-horizon quadratic-programming approach to the signal control problem in large-scale congested urban road networks," *Transportation Research Part C: Emerging Technologies*, vol. 18, no. 5, pp. 680–694, 2010.

[4] A. Kouvelas, K. Aboudolas, M. Papageorgiou, and E. B. Kosmatopoulos, "A hybrid strategy for real-time traffic signal control of urban road networks," *IEEE Transactions on Intelligent Transportation Systems*, vol. 12, no. 3, pp. 884–894, 2011.

[5] L. Tassiulas and A. Ephremides, "Stability properties of constrained queueing systems and scheduling policies for maximum throughput in multihop radio networks," *IEEE Transactions on Automatic Control*, vol. 37, no. 12, pp. 1936–1948, 1992.

[6] P. Varaiya, "Max pressure control of a network of signalized intersections," *Transportation Research Part C: Emerging Technologies*, vol. 36, pp. 177–195, 2013.

[7] A. Kouvelas, J. Lioris, S. Fayazi, and P. Varaiya, "Maximum pressure controller for stabilizing queues in signalized arterial networks," *Transportation Research Record: Journal of the Transportation Research Board*, no. 2421, pp. 133–141, 2014.

[8] T. Wongpiromsarn, T. Uthaicharoenpong, Y. Wang, E. Frazzoli, and D. Wang, "Distributed traffic signal control for maximum network throughput," in *15th International IEEE Conference on Intelligent Transportation Systems*. IEEE, 2012, pp. 588–595.

[9] A. A. Zaidi, B. Kulcsar, and H. Wymeersch, "Traffic-adaptive signal control and vehicle routing using a decentralized back-pressure method," in *European Control Conference*. IEEE, 2015, pp. 3029–3034.

[10] N. Geroliminis and C. F. Daganzo, "Existence of urban-scale macroscopic fundamental diagrams: Some experimental findings," *Transportation Research Part B: Methodological*, vol. 42, no. 9, pp. 759–770, 2008.

[11] J. Godfrey, "The mechanism of a road network," *Traffic Engineering and Control*, vol. 11, no. 7, pp. 323–327, 1969.

[12] C. F. Daganzo, "Urban gridlock: Macroscopic modeling and mitigation approaches," *Transportation Research Part B: Methodological*, vol. 41, no. 1, pp. 49–62, 2007.

[13] M. Keyvan-Ekbatani, A. Kouvelas, I. Papamichail, and M. Papageorgiou, "Exploiting the fundamental diagram of urban networks for feedback-based gating," *Transportation Research Part B: Methodological*, vol. 46, no. 10, pp. 1393–1403, 2012.

[14] V. V. Gayah, X. S. Gao, and A. S. Nagle, "On the impacts of locally adaptive signal control on urban network stability and the macroscopic fundamental diagram," *Transportation Research Part B: Methodological*, vol. 70, pp. 255–268, 2014.

[15] J. Haddad and A. Shraiber, "Robust perimeter control design for an urban region," *Transportation Research Part B: Methodological*, vol. 68, pp. 315–332, 2014.

[16] J. Haddad and N. Geroliminis, "On the stability of traffic perimeter control in two-region urban cities," *Transportation Research Part B: Methodological*, vol. 46, no. 9, pp. 1159–1176, 2012.

[17] K. Aboudolas and N. Geroliminis, "Perimeter and boundary flow control in multi-reservoir heterogeneous networks," *Transportation Research Part B: Methodological*, vol. 55, pp. 265–281, 2013.

[18] N. Geroliminis, J. Haddad, and M. Ramezani, "Optimal perimeter control for two urban regions with macroscopic fundamental diagrams: A model predictive approach," *IEEE Transactions on Intelligent Transportation Systems*, vol. 14, no. 1, pp. 348–359, 2013.

[19] M. Hajiahmadi, J. Haddad, B. De Schutter, and N. Geroliminis, "Optimal hybrid perimeter and switching plans control for urban traffic networks," *IEEE Transactions on Control Systems Technology*, vol. 23, no. 2, pp. 464–478, 2015.

[20] J. Haddad, M. Ramezani, and N. Geroliminis, "Cooperative traffic control of a mixed network with two urban regions and a freeway," *Transportation Research Part B: Methodological*, vol. 54, pp. 17–36, 2013.

[21] M. Ramezani, J. Haddad, and N. Geroliminis, "Dynamics of heterogeneity in urban networks: aggregated traffic modeling and hierarchical control," *Transportation Research Part B: Methodological*, vol. 74, pp. 1–19, 2015.

[22] M. Yildirimoglu, M. Ramezani, and N. Geroliminis, "Equilibrium analysis and route guidance in large-scale networks with MFD dynamics," *Transportation Research Part C: Emerging Technologies*, vol. 59, pp. 404–420, 2015.

[23] M. Hajiahmadi, V. L. Knoop, B. De Schutter, and H. Hellendoorn, "Optimal dynamic route guidance: A model predictive approach using the macroscopic fundamental diagram," in *16th International IEEE Conference on Intelligent Transportation Systems*. IEEE, 2013, pp. 1022–1028.

[24] J. Andersson, "A General-Purpose Software Framework for Dynamic Optimization," PhD thesis, Arenberg Doctoral School, KU Leuven, Department of Electrical Engineering (ESAT/SCD) and Optimization in Engineering Center, Kasteelpark Arenberg 10, 3001-Heverlee, Belgium, October 2013.

[25] A. Wächter and L. T. Biegler, "On the implementation of an interior-point filter line-search algorithm for large-scale nonlinear programming," *Mathematical Programming*, vol. 106, no. 1, pp. 25–57, 2006.

[26] M. Ben-Akiva and M. Bierlaire, "Discrete choice methods and their applications to short term travel decisions," in *Handbook of Transportation Science*. Springer, 1999, pp. 5–33.